Inorganica Chimica Acta, 126 (1987) 113–117

Preparation, Crystal Structure and Thermal Behaviour of Bischromatodihydroxobis-(pyridine)tricopper(II) $[Cu_3(CrO_4)_2(OH)_2(C_5H_5N)_2]$

WOLFGANG BENSCH, NIKOLAOS SEFERIADIS and HANS R. OSWALD

Institute for Inorganic Chemistry, University of Zurich, Winterthurerstrasse 190, CH-8057 Zurich, Switzerland

(Received June 28, 1986; revised August 19, 1986)

Abstract

The title compound was prepared by slow crystallization from a hot aqueous solution of copper(II)-dichromate and pyridine. The structure determination was performed at room temperature on a single crystal in the triclinic space group $P\bar{1}$, $a = 5.378(1)$, $b = 5.619(1)$, $c = 13.569(2)$ Å, $\alpha = 93.32(1)$, $\beta = 100.25(1)$, $\gamma = 98.45(1)°$. Using 2026 reflections with $F_o^2 > \sigma(F_o^2)$ obtained on a CAD-4 single crystal diffractometer the structure was solved by conventional Patterson and Fourier methods and full matrix least-squares refinement to $R = 0.047$. The structure consists of complex chains built up from two different (4 + 2) distorted copper(II) octahedra sharing common edges. These chains are linked via O–Cr–O bonds thus forming a two-dimensional infinite network. The pyridine rings extending into the space between these layers are disordered due to rotation around the Cu–N bond. In the course of the refinement two favoured positions with occupation probabilities 50:50 percent were found. During thermal decomposition the compound loses pyridine and water followed by a release of oxygen to yield polycrystalline $CuCr_2O_4$ and CuO. An intermediate phase with empirical formula $Cu_3O(CrO_4)_2$ was detected by X-ray powder diffraction and its unit cell parameters were determined.

Introduction

Copper chromites are industrially important catalysts for the selective hydrogenation of functional groups in aliphatic and aromatic compounds and also for the conversion of carbon monoxide to carbon dioxide. During our investigations on the preparation of catalytically active mixed metal oxides at moderate temperatures from solid state precursors containing Cu and Cr in several atomic ratios, we obtained the title compound, which is to our knowledge new, and studied its structure and thermal decomposition behaviour on single crystals.

Experimental

Preparation

A 0.1 molar aqueous solution of $CuCr_2O_7$ obtained by reacting $Cu_2CO_3(OH)_2$ with chromic acid yields with an excess of pyridine the light green complex $CuCr_2O_7 \cdot 4$(pyridine) [1, 2]. By treatment of this precipitate with water at about 80 °C, the title compound could be obtained as very thin, light brown, irregularly contoured single crystalline lamellae within a few days. After washing with ethanol and ether, they were dried at ambient temperature. The product remains stable on air. Its composition was determined by the usual analytical methods.

Crystal Data and Structure Refinement

$C_{10}H_{12}Cr_2Cu_3N_2O_{10}$, $M = 614.84$, triclinic, space group $P\bar{1}$, $a = 5.378(1)$, $b = 5.619(1)$, $c = 13.569(2)$ Å, $\alpha = 93.32(1)$, $\beta = 100.25(1)$, $\gamma = 98.45(1)°$, $V = 397.6(2)$ Å^3, $Z = 1$, $F(000) = 301$, $D_{calc} = 2.568$ g cm^{-3}, λ(Mo Kα) = 0.7107 Å, $\mu = 53.1$ cm^{-1}. A single crystal of approximate dimensions 0.13 × 0.14 × 0.01 mm was centered on an Enraf Nonius CAD-4 four circle diffractometer. Unit cell parameters as well as crystal orientation were determined from least-squares refinement of 25 automatically centered reflections in the range $11° < \theta < 22°$. A data set was collected (ω–2θ scans) using graphite monochromated Mo Kα radiation, max $\theta = 30°$; h:−9 to 9, k:−10 to 10, l:0 to 22. Intensity and orientation control reflections monitored at regular intervals showed no significant changes. The data reduction procedure led to 3484 unique data. Lorentz, polarization and isotropic extinction corrections were applied, but not for absorption. The structure was solved by Patterson and Fourier techniques and refined by full matrix least-squares calculations using finally anisotropic temperature factors. After location of the metal and oxygen atoms one pyridine ring appeared in the difference Fourier synthesis (ΔF). The ring was refined without constraints. The isotropic temperature factors of the carbon and nitrogen atoms were relatively high, whereas those of the other

0020-1693/87/$3.50

atoms were normal. In the ΔF synthesis a second ring occurred with the nitrogen and *para* standing carbon atom at nearly the same positional parameters as in the first pyridine. The planes of the two rings build a dihedral angle of 120°. In the early stages the two pyridines were treated as follows: for both rings common N and *para* standing C atoms were refined. The site occupation factors of the other C atoms were refined with a common free variable leading to occupation probabilities of 48:52. Since the C–C and C–N distances in the rings are rather unreliable we decided to fit a regular pyridine (data taken from ref. 3) to the positional parameters of our rings. The idealized pyridines were treated as rigid bodies. Finally all atoms were refined anisotropically, the site occupation factors of the ring atoms with a common free variable to 50:50. This procedure led to 0.047 and 0.051 for R and R_w respectively, using 2026 data with $F_o^2 > \sigma(F_o^2)$. The weighting scheme $w = k/(\sigma^2(F) + 0.00065F^2)$ (k refined to 1.13) showed no dependence of the function minimized upon $(\sin\theta/\lambda)$ or the magnitude of F. At convergence (Δ/σ) became $\leqslant 0.006$. The final difference Fourier synthesis showed 1.4 $e^-/Å^3$ near Cu(2) and -1.3 $e^-/Å^3$ as hole. Anomalous dispersion corrections were applied for all atoms. It should be stressed here that long exposed zero and first layer Weissenberg photographs gave no indication for a superstructure. Final atomic coordinates as well as isotropic thermal parameters are summarized in Table I. Scattering factors and correction parameters were taken from ref. 4. Programs used: SHELX-76 [5], PARST7 [6] and SHELXTL (for the fitting procedure) [7] See also 'Supplementary Material'.

TABLE I. Positional and Isotropic Thermal Parameters[a] ($Å^2$) for $Cu_3(CrO_4)_2(OH)_2(C_5H_5N)_2$

Atom	x/a	y/b	z/c	U_{eq}
Cu(1)	0.8185(1)	0.4846(1)	0.8997(1)	0.012(1)
Cu(2)	1.0000(0)	0.0000(0)	1.0000(0)	0.013(1)
Cr	0.6215(2)	0.1517(2)	0.1526(1)	0.012(1)
O(1)	1.1094(6)	0.3316(6)	0.9647(3)	0.013(3)
O(2)	1.0925(7)	0.8466(6)	0.8835(3)	0.016(3)
O(3)	0.4852(7)	0.5869(7)	0.8742(3)	0.018(3)
O(4)	0.5863(8)	0.0754(7)	0.9039(3)	0.021(4)
O(5)	0.6618(8)	0.1327(8)	0.2714(3)	0.026(4)
N(1)	0.825(2)	0.397(2)	0.756(1)	0.018(10)
C(1)	0.859(2)	0.179(2)	0.719(1)	0.022(9)
C(2)	0.851(2)	0.122(2)	0.618(1)	0.033(12)
C(3)	0.804(2)	0.289(2)	0.551(1)	0.034(14)
C(4)	0.767(2)	0.510(2)	0.587(1)	0.033(11)
C(5)	0.781(2)	0.557(2)	0.689(5)	0.026(10)
N(1')	0.789(2)	0.366(2)	0.756(1)	0.010(9)
C(1')	0.576(2)	0.366(2)	0.690(1)	0.021(9)
C(2')	0.549(2)	0.293(2)	0.589(1)	0.030(11)
C(3')	0.750(2)	0.220(2)	0.553(1)	0.030(14)
C(4')	0.972(2)	0.221(2)	0.620(1)	0.035(13)
C(5')	0.986(2)	0.293(2)	0.720(1)	0.023(10)

[a] Equivalent isotropic temperature factors defined as one third of the trace of the orthogonalized U tensor.

Thermal Analysis

The thermal analyses were performed using small samples (<5 mg) of single crystals on a Perkin-Elmer TGS-2 device. *In situ* analyses of the evolved gases were made with a coupled mass spectrometer (Balzers QMG-511). Diffraction patterns as a function of temperature and time were recorded on a Guinier Lenné heating camera. A powder diffraction pattern of the intermediate phase $Cu_3O(CrO_4)_2$ was recorded on a Siemens D 500 diffractometer using Cu Kα radiation.

Discussion

The Structural Analysis

A packing diagram of the structure is displayed in Fig. 1 and the environment of the copper atoms is shown in Fig. 2. Only one of the two favoured positions of the disordered pyridine rings is drawn in Figs. 1 and 2. The bond distances and angles are listed in Table II. As can be seen from the respective illustration two Cu(1)-octahedra are linked by a common edge. These pairs of octahedra are joined to the adjacent pairs on opposite sides by Cu(2)-octahedra sharing common edges. This arrangement leads to complex chains of edge sharing octahedra. These chains are linked via O–Cr–O bonds thus forming a two-dimensional infinite network parallel to a-b, the pronounced plane of the single crystalline lamellae. The pyridine rings extend into the space between these layers. From chemical and structural considerations the oxygen atom denoted as O(1) should be the oxygen of the hydroxide group. This atom is bound to 3 Cu atoms simultaneously. The oxygen atom O(5) is only bound to the chromium atom. The distances O(1)–O(5), however, are too long to postulate O(1)–H···O(5) hydrogen bonds, but there exists a contact of 2.808(5) Å between O(1) and O(3) at a neighbouring octahedron which is compatible with a hydrogen bridge. The copper to ligand distances range from 1.941(4) to 2.459(4) Å for the Cu(1)-octahedron and from 1.934(4) to 2.478(4) Å for the Cu(2)-octahedron. As typical for the Jahn-Teller ion Cu^{2+}, two distances are significantly longer than the other Cu–ligand bonds (see Table II). As can be deduced from the angles O–Cu(1)–O resp. –N and O–Cu(2)–O the Cu(1)-octahedron is more distorted. The shortest distance between copper atoms in neighbouring octahedra is 3.034(1) Å. This relatively short metal to metal distance is caused by a small displacement of the Cu atoms from the center of the octahedra towards each other. The environment of the chromium atom is rather normal. As expected the Cr–O(5) distance is shorter than the other Cr–O

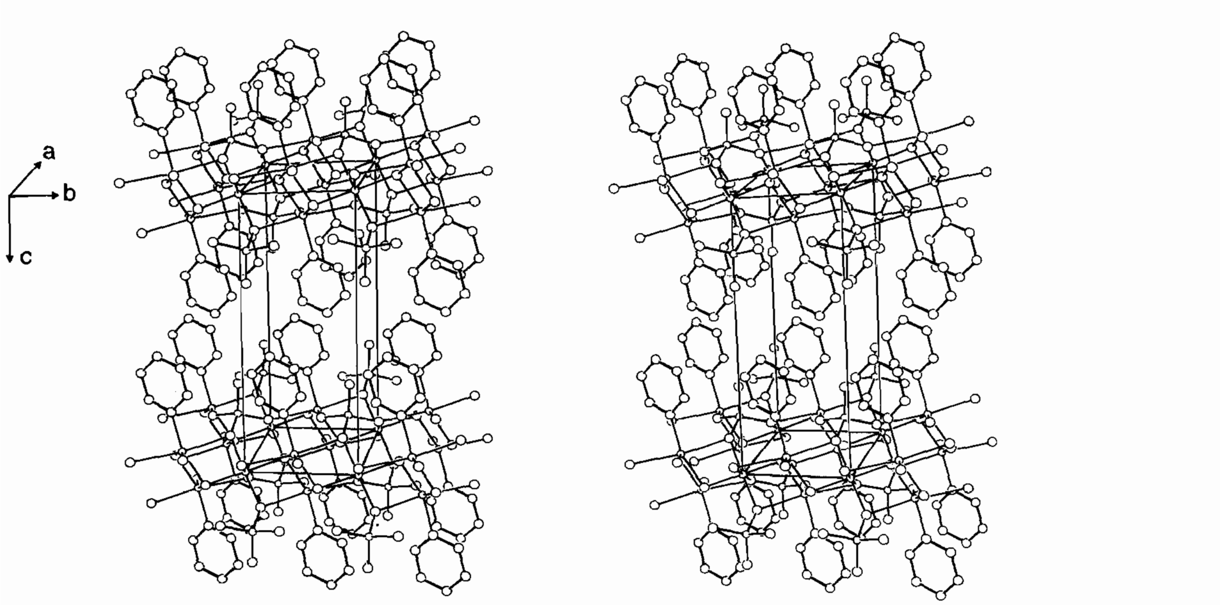

Fig. 1. Stereoscopic diagram of the contents of the unit cell for $[Cu_3(CrO_4)_2(OH)_2(C_5H_5N)_2]$.

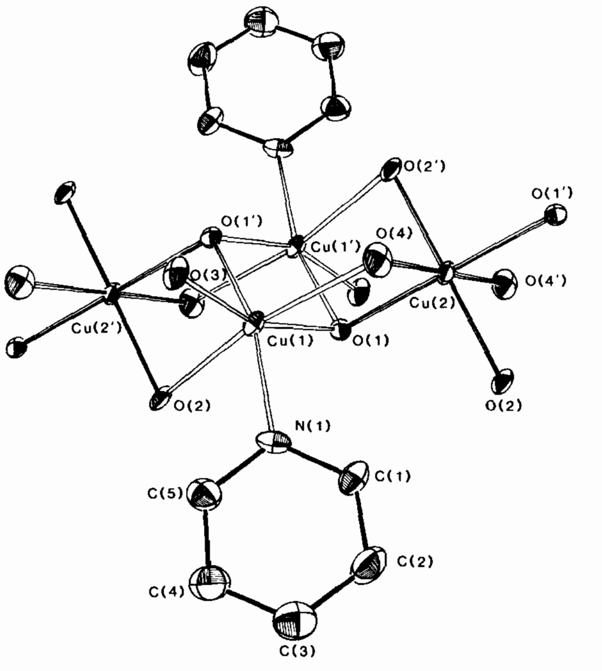

Fig. 2. The environment of the two different copper atoms in $[Cu_3(CrO_4)_2(OH)_2(C_5H_5N)_2]$. Thermal ellipsoids are drawn at the 75% probability level.

distances. The pyridine rings were treated as rigid bodies during the crystal structure refinement. Therefore a discussion of the bond distances and angles is unnecessary. A dihedral angle of 120° between the two pyridine least squares planes is calculated. A reason for the disorder of the pyridine rings may be the fact that there is no steric hindrance for rotation about the Cu–N bond.

TABLE II. Selected Bond Distances (Å) and Angles (°)

Cu(1)–Cu(1')	3.034(1)	
Cu(1)–Cu(2)	3.310(1)	
Cu(1)–Cu(2')	3.071(1)	
Cu(1)–N(1)	1.987(5)	
Cu(1)–O(1)	1.989(3)	
Cu(1)–O(1')	2.002(3)	
Cu(1)–O(2)	2.376(3)	
Cu(1)–O(3)	1.941(4)	
Cu(1)–O(4)	2.459(4)	
Cu(2)–O(1)	1.982(3)	2x
Cu(2)–O(2)	1.934(4)	2x
Cu(2)–O(4)	2.478(4)	2x
Cr–O(2)	1.694(4)	
Cr–O(3)	1.689(4)	
Cr–O(4)	1.621(4)	
Cr–O(5)	1.600(4)	
N(1)–C(1)	1.34(1)	
N(1)–C(5)	1.35(1)	
C(1)–C(2)	1.37(1)	
C(2)–C(3)	1.37(1)	
C(3)–C(4)	1.37(1)	
C(4)–C(5)	1.37(1)	
O(1)–Cu(1)–O(1')	81.1(2)	
O(1)–Cu(1)–O(2)	92.5(1)	
O(1)–Cu(1)–O(3)	160.1(2)	
O(1)–Cu(1)–O(4)	81.3(1)	
O(1)–Cu(1)–N(1)	99.6(3)	
O(1')–Cu(1)–O(2)	74.7(1)	
O(1')–Cu(1)–O(3)	89.0(2)	
O(1')–Cu(1)–O(4)	111.3(1)	
O(1')–Cu(1)–N(1)	161.0(3)	
O(2)–Cu(1)–O(3)	101.5(1)	
O(2)–Cu(1)–O(4)	170.3(1)	

(continued)

TABLE II. *(continued)*

O(2)–Cu(1)–N(1)	86.3(2)
O(3)–Cu(1)–O(4)	86.5(1)
O(3)–Cu(1)–N(1)	95.5(3)
O(4)–Cu(1)–N(1)	87.5(2)
O(1)–Cu(2)–O(4)	80.9(1)
O(1)–Cu(2)–O(2')	86.1(2)
O(4)–Cu(2)–O(2')	86.9(1)
O(2)–Cr–O(3)	109.0(2)
O(2)–Cr–O(4)	111.1(2)
O(2)–Cr–O(5)	108.5(2)
O(3)–Cr–O(4)	110.0(2)
O(3)–Cr–O(5)	109.1(2)
O(4)–Cr–O(5)	109.2(2)
C(1)–N(1)–C(5)	115.5(6)
N(1)–C(1)–C(2)	123.5(7)
C(1)–C(2)–C(3)	119.8(7)
C(2)–C(3)–C(4)	117.7(6)
C(3)–C(4)–C(5)	119.6(7)
N(1)–C(5)–C(4)	123.9(8)

The standard deviations of the last significant digits are given in parentheses.

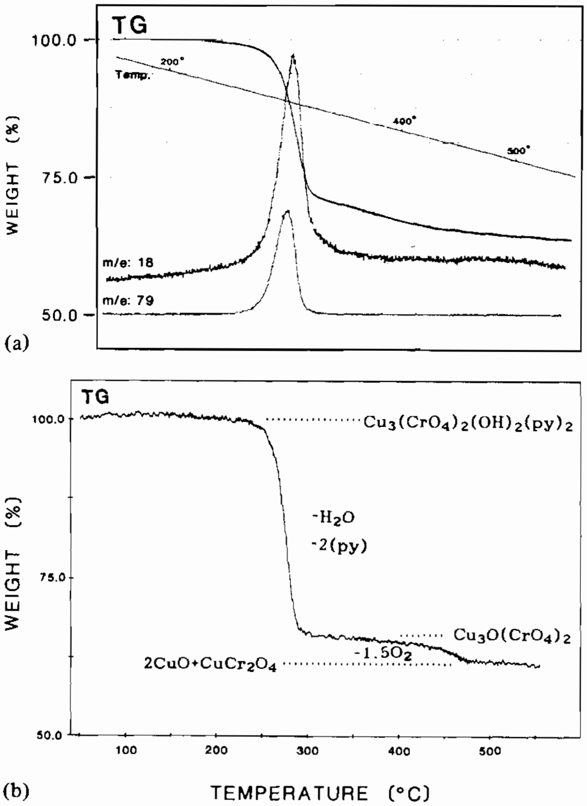

Fig. 3. Thermal behaviour of $[\mathrm{Cu_3(CrO_4)(OH)_2(C_5H_5N)_2}]$. (a) Combined TG/MS curves for decomposition in nitrogen atmosphere, flush 30 ml/min, 3.17 mg sample, heating rate 10 °C/min (intensities of the MS curves are in arbitrary scale). (b) TG curve for decomposition in air, flush 30 ml/min, 0.60 mg sample, heating rate 10 °C/min.

Thermal Behaviour

The combined thermogravimetric and mass spectrometry measurements are illustrated in Fig. 3a. The course of the decomposition in a nitrogen atmosphere can be summarized by the following sequence of steps, which are consistent with the observed weights of the intermediate and final materials, expressed as a percentage of the initial weight (calculated values in parentheses)

$$\underset{100\%}{\mathrm{Cu_3(CrO_4)_2(OH)_2(py)_2}} \xrightarrow[\substack{-\mathrm{H_2O} \\ -2(\mathrm{py})}]{220-320\ ^\circ\mathrm{C}}$$

$$\underset{71.5\ (71.3)\%}{\mathrm{Cu_3O(CrO_4)_2}} \xrightarrow[-1.5\ \mathrm{O_2}]{320-550\ ^\circ\mathrm{C}} \underset{63.4\ (63.7)\%}{\mathrm{2CuO + CuCr_2O_4}}$$

Pyridine and water were identified by mass spectrometry during decomposition (Fig. 3a). According to a comparison of Figs. 3a and b, the decomposition behaviour of the title compound is, in principle, independent from the flush gas used. The step corresponding to the intermediate phase $\mathrm{Cu_3O(CrO_4)_2}$ is, however, better resolved upon heating in air. Guinier–Lenné X-ray photographs during decomposition revealed a nearly amorphous character of the intermediate phase if it was formed under nitrogen, but sharp reflections if the decomposition took place in air under otherwise the same conditions. The powder pattern of the intermediate phase could not be attached to data of Cu–Cr oxidic phases taken from the literature. The final products were also crystalline. The diagram of $\mathrm{CuCr_2O_4}$ coincides with the data for the high temperature cubic modification given in JCPDS: 26-509. A larger quantity of $\mathrm{Cu_3O(CrO_4)_2}$ could be obtained by an isothermal heat treatment of the title compound at 350 °C in air. The heating rate up to this temperature must be very low. Upon heating too fast a burst-like reaction takes place.

The diffraction pattern (Fig. 4) of $\mathrm{Cu_3O(CrO_4)_2}$ could be indexed on the base of an orthorhombic unit cell with $a = 7.418$, $b = 14.322$ and $c = 6.663$ Å using the VISSER program [8]. The lattice parameters were also refined with this program. From similarities between the stoichiometries as well as the unit cell parameters, it can be assumed that our intermediate phase $\mathrm{Cu_3O(CrO_4)_2}$ resp. $\mathrm{Cu_3Cr_2O_9}$ is isotypic with the compound $\mathrm{Cu_3Mo_2O_9}$, space group $Pna2_1$ [9]. Investigations for the preparation of single crystals of the intermediate phase are in progress.

Supplementary Material

Observed and calculated structure factors as well as the anisotropic temperature factors are available from the Editor on request.

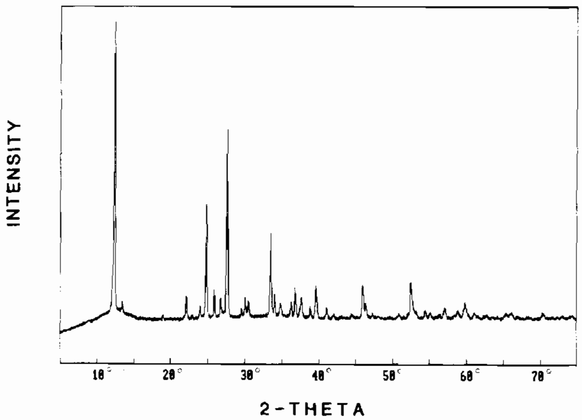

Fig. 4. Powder diffractogram of the intermediate phase $Cu_3O(CrO_4)_2$, measured in reflection with Cu Kα (intensities in arbitrary scale).

Acknowledgements

We gratefully acknowledge the help of P. Hug for TG/MS measurements, the support of Dr. R. Prewo in using the SHELXTL program, and financial means provided by the Swiss National Science Foundation under Project No. 2.023-083.

References

1 N. Parravano and A. Pasta, *Gazz. Chim. Ital., 37,* 252 (1907).
2 S. H. C. Briggs, *Z. Anorg. Allg. Chem., 56,* 246 (1908).
3 Naiyin Li, V. Petricek, P. Coppens and J. Landrum, *Acta Crystallogr., Sect. C, 41,* 902 (1985).
4 'International Tables for X-ray Crystallography', Vol. III, Kynoch Press, Birmingham, 1965.
5 G. M. Sheldrick, 'SHELX-76', program for crystal structure determination, University of Cambridge, U.K., 1976.
6 M. Nardelli, 'PARST7', programs for crystallographic calculations, Parma, 1981.
7 G. M. Sheldrick, 'SHELXTL', an integrated system for solving, refining and displaying crystal structures from diffraction data, 1980 and 1983.
8 J. W. Visser, *J. Appl. Crystallogr., 2,* 89 (1969); a fully automatic program for finding the unit cell from powder data.
9 L. Kihlborg, R. Norrestam and B. Olivecrona, *Acta Crystallogr., Sect. B, 27,* 2066 (1971).